ASTER GDEM V3
(ASTER Global DEM)

Japan's Ministry of Economy, Trade, and Industry (METI)

National Aeronautics and Space Administration (NASA)

Jet Propulsion Laboratory/California Institute of Technology

Prepared by Michael Abrams and Robert Crippen

User Guide

Version 1

July 2019

ASTER Global DEM (ASTER GDEM)

Quick Guide for V3

1. Introduction

The Advanced Spaceborne Thermal Emission and Reflection Radiometer (ASTER) instrument that was launched onboard NASA's Terra spacecraft in December 1999 has an along-track stereoscopic capability using its near infrared spectral band to acquire the stereo data. ASTER has two telescopes, one for nadir-viewing and another for backward-viewing, with a base-to-height ratio of 0.6. The spatial resolution is 15 meters (m) in the horizontal plane. Each scene consists of 4,100 samples by 4,200 lines which corresponds to about 60 kilometers (km) by 60 km ground area.

The ASTER Global Digital Elevation Model (ASTER GDEM) Version 3 (V3) was generated using 1,880,306 Level-1A scenes acquired between March 1, 2000 and November 30, 2013. ASTER GDEM was created by stacking all individual cloud-masked scene DEMs and non-cloud-masked scene DEMs, then applying various algorithms to remove abnormal data [1], [2], [3].

A statistical approach is not always effective for anomaly removal in areas with a limited number of images. Several existing reference DEMs were used to replace residual anomalies caused by the insufficient number of stacked scenes.

In addition to ASTER GDEM, the ASTER Global Water Body Database (ASTWBD) was generated as a by-product to correct elevation values of water body surfaces like sea, rivers, and lakes. The ASTWBD was applied to GDEM to provide proper elevation values for water body surfaces. The sea and lake have a flattened elevation value. The river has a stepped-down elevation value from the upper stream to the lower stream.

2. Data Product Files

Each ASTER GDEM tile has two associated files: a DEM file with elevation information and a quality assessment (QA) NUM file. Both files have a dimension of 3601 samples by 3601 lines, which corresponds to 1 degree by 1 degree data area. The names of individual data tiles refer to the latitude and longitude at the geometric center of the lower-left (southwest) corner pixel. For example, the coordinates of the lower-left corner of the tile ASTGTMV003_N00E006 tile are 0 degree north latitude and 6 degrees east longitude. ASTGTMV003_N00E006_dem and ASTGTMV003_N00E006_num files accommodate DEM and QA data, respectively. The rows at the north and south edges as well as the column at the east and west edges of each cell overlap and are identical to the edge row and column in the adjacent cell.

The data coverage is north 83 degrees to south 83 degrees. The GDEM collection includes 22,912 tiles.

3. Data Product Characteristics

Data product characteristics are summarized in Table 1.

Table 1. Data characteristics

Tile Size	3601 x 3601 (1 degree by 1 degree)
Posting interval	1 arc-second (30 m)
Geographic coordinates	Geographic latitude and longitude
DEM output format	DEM: GeoTiff, signed 16 bits, and 1m/DN for DEM; NUM: GeoTiff; unsigned 8 bit number of individual scenes used to compile each pixel (maxed at 50); and source of fill for missing ASTER data (see index below)
Special DN values	-9999 for void pixels and 0 for sea-level water body
Ellipsoid/Geoid	Referenced to the WGS84/EGM96 geoid
Coverage	North 83 degrees to south 83 degrees, 22,912 tiles for GDEM

4. Anomaly Correction

4.1 Initial Corrections

A cloud masking and the statistical approach were used to select the effective data for stacking. Cloud masking cannot completely remove the clouds. In addition, the statistical approach is not always effective for anomaly removal in the cases where a small number of scenes were used. At least three stacked scenes are necessary to apply statistical algorithms.

Existing DEMs were used as reference data to correct and replace anomalies or missing data. Table 2 shows the list of the reference DEMs used for ASTER GDEM V3 data. The anomaly data were filled with the reference data according to the priority for usage shown in Table 2. When using Global Multi-resolution Terrain Elevation Data 2010 (GMTED2010) 7.5 sec reference data, only an anomaly larger than 1 km² was filled with the reference data. Smaller size anomalies less than1 km² were filled with two dimensional interpolation from the perimeter data.

The reference data shown in Table 2 collectively cover all ASTER GDEM voids. All of these reference data are not anomaly free, but the initial ASTER GDEM V3 was nearly void free except for Greenland and Antarctica.

Table 2. Reference DEM list

SRTM1 V3 [4] (First priority)	Posting: 1 arc-second Coverage: North 60 degrees to south 56 degrees
Alaska DEM [5] (Second priority)	Posting: 2 x 2 arc-seconds Coverage: All Alaska territory
CDED* [6] (Canadian Digital Elevation Dataset)	Posting: 3 arc-seconds for latitude 3, 6 and 12 arc-seconds for longitude depending on latitude Coverage: All Canada territory

(Second priority)	
GMTED2010 [7] (Third priority)	Posting: 7.5 arc-seconds Coverage: North 84 degrees to south 56 degrees (except Greenland)

4.2 Final Correction

4.2.1 GDEM Error Mask Generation

The GDEM error mask was created in three major steps. First, the input GDEM, described above, (both Version 2 and Version 3) was compared to Shuttle Radar Topography Mission (SRTM) [4] and PRISM (30 m DEM available from the Japan Aerospace Exploration Agency (JAXA), created from Advanced Land Observing Satellite (ALOS) Panchromatic Remote-sensing Instrument for Stereo Mapping (PRISM) optical data [8]) for reasonable consistency. Second, the input GDEM was evaluated for the likelihood of errors (such as clouds) based upon its own morphology. Third, the composite mask generated from the first and second steps was expanded by filtering to better include all input GDEM error pixels.

The first step followed qualitative logical probabilities. SRTM has no cloud errors, and the cloud avoidance for PRISM appears to be more consistently effective than the cloud avoidance of the input GDEM. However, both SRTM and PRISM have data voids, so are not always available for comparison with the input GDEM. Also, SRTM can have interferometric unwrapping errors, although the most significant of those were likely detected and were voided prior to comparison to the input GDEM (see above). In short, SRTM is generally considered reliable and PRISM is considered less error-prone than the input GDEM, especially where two or fewer ASTER scenes were used to create GDEM. With that in mind, this first step in creating the GDEM error mask adhered to the following logic:

1. SRTM and PRISM not void: Input GDEM pixel was rejected if it differed from both SRTM and PRISM by more than 80 m.

2. SRTM and PRISM both void: Input GDEM not rejected.

3. SRTM void but PRISM not void: Input GDEM was rejected if more than 80 m different from PRISM, unless input GDEM NUM (number) pixel value was 3 or more.

4. PRISM void but SRTM not void: Input GDEM was rejected if more than 80 m different from SRTM.

An initial rejection mask was thus created. The 80 m threshold was determined empirically from extensive experience worldwide, maximizing cloud masking while minimizing the loss of obviously real topography such as dendritic erosion patterns. The mask was then expanded to the eight neighboring pixels of any masked pixel in order to more assuredly include problem areas in the mask.

In the second major step, the mask was then additionally expanded to any pixel that differed "too much" from any neighboring pixel (thus having a slope so high as to be more likely an error, such as a cloud edge, than to be natural topography). The threshold for "too much" was defined as greater than 100 m in the north-south or east-west direction at the equator, and it was defined as 141 m (about the square root of 2 times 100) in the northwest-southeast and northeast-southwest directions at the equator. Exceeding the threshold in any direction resulted in GDEM pixel masking. The threshold was

decreased appropriately as a cosine function of latitude for all orientations (except north-south) because longitude 1arc-second pixel spacings decrease with latitude. The (by-chance) round number 100 was (again) determined empirically. Lower thresholds lost too much good topography and higher thresholds accepted too many cloud errors.

At this point a mask had been created based upon two major steps: (1) comparisons of individual pixels to themselves in other datasets, and (2) comparisons of individual GDEM pixels to their immediate GDEM neighbors. Neither of these steps "look" across significant geography which was found to be a problem. Often edges of clouds were masked but not the cloud interiors (which could be much less steep). Thus, a third step, spatial filtering, was needed to "fill-in" the mask.

Extensive testing resulted in an effective filtering method, as follows. Any non-masked pixel was added to the mask if masked pixels were found within a 50-pixel radius in at least 12 of 16 "spoke" directions (north, north-northwest, northwest, west-northwest, west, etc.). The concept here is that small areas need to be additionally masked if they are enclosed by masked pixels or if they are almost (at least 12/16) enclosed by masked pixels. Note that this method does not expand the exterior edges of masked regions (i.e., areas clearly exterior to clouds are preserved as unmasked).

A 5 by 5 median filter of the binary mask (masked versus not masked pixels) was needed to avoid some noise from the 16 detector "spokes". Previously identified "too steep" pixels were then restored to the mask where eliminated by the 5 by 5 median filter. The mask was then complete and found to be extremely effective.

4.2.2 GDEM Void Filling

The masking of errors in GDEM creates voids that need to be filled. Preferably these voids are filled with an alternative DEM rather than via interpolation. For consistency, the best DEM to fill the latest GDEM is an earlier GDEM. That results in a final GDEM that is maximally from ASTER and thus most inherently an ASTER product with minimum elevation data from other sources. Using GDEM V2 to fill voids is possible because errors in GDEM V3 were not always spatially coincident with errors in GDEM V2. The newer GDEM uses the ASTER scenes used in GDEM V2 plus additional (more recent) scenes. In general, having more scenes results in fewer errors. However, inclusion of additional cloudy scenes occasionally introduced errors that did not occur in the older GDEM.

Thus, GDEM V2 was the first choice as the elevation model for filling voids of the newer GDEM. Since GDEM V2 has errors too, the same error masking procedure (above) was applied. SRTM, where available, was the elevation model of second choice to be used as fill. This was the reprocessed (e.g. ICESat adjusted) SRTM that was concurrently (circa 2017) generated for the NASADEM Project. The original SRTM had been the primary fill for all prior versions of GDEM. As described above, some interferometric unwrapping errors were removed from SRTM but no further masking was applied. PRISM ALOS World 3D-30m (AW3D30), where available, was used as third choice, after it was subjected to a masking routine similar to that applied to the GDEM elevation models. Masking PRISM AW3D30 was a precautionary step. Note that after masking GDEM V2, all of the filler elevation models had voids (GDEM V2, SRTM, and PRISM AW3D30), either inherently, or from masking, or both.

The void fill routine is a modified version of the Delta Surface Fill method of Grohman [9]. The published method was modified in order to (1) use filler DEMs with voids, (2) reduce the spread of errors from void edges into the void fill, and (3) improve processing speed. (See Appendix 1 for further details of the modified procedure).

With the delta surface calculated and filled, each intermediate DEM (from each filling step) is generated such that (1) the output is the primary DEM where it exists, (2) the output is void where both DEMs are void and (3) the output is the secondary DEM shifted by the filled delta surface where the primary DEM is void and the secondary DEM is not void.

To summarize, the initial GDEM V3, the GDEM V2, and the PRISM DEM were error-masked via select comparisons to each other and to SRTM. The masks were then expanded to also remove DEM morphologies more likely to be clouds (and other errors) than real terrain. Specially designed filtering improved the masks. Voids in the masked initial GDEM V3 were then sequentially filled with the masked GDEM V2, SRTM, and the masked PRISM DEM (in that order). Interpolation filled any remaining voids. Results for all quads outside Antarctica and Greenland were visually inspected and found to be satisfactory to excellent, with some exceptions. Results for major ice sheets (often with few ASTER scene inputs) often have poor quality and limited utility.

An example of the results of the procedure is shown in Figure 1. A 400 by 400 pixel subarea of tile N60E05 was processed using the above process. The input was the GDEM provided by the contractor, who applied some additional void-filling corrections that introduced new artifacts (left image), partially due to use of poor quality Global Multi-resolution Terrain Elevation Data 2010 (GMTED 2010) data. The right image shows the final, fully corrected GDEM V3 tile. Note that his area is above 60 degrees north latitude, where there are no SRTM data.
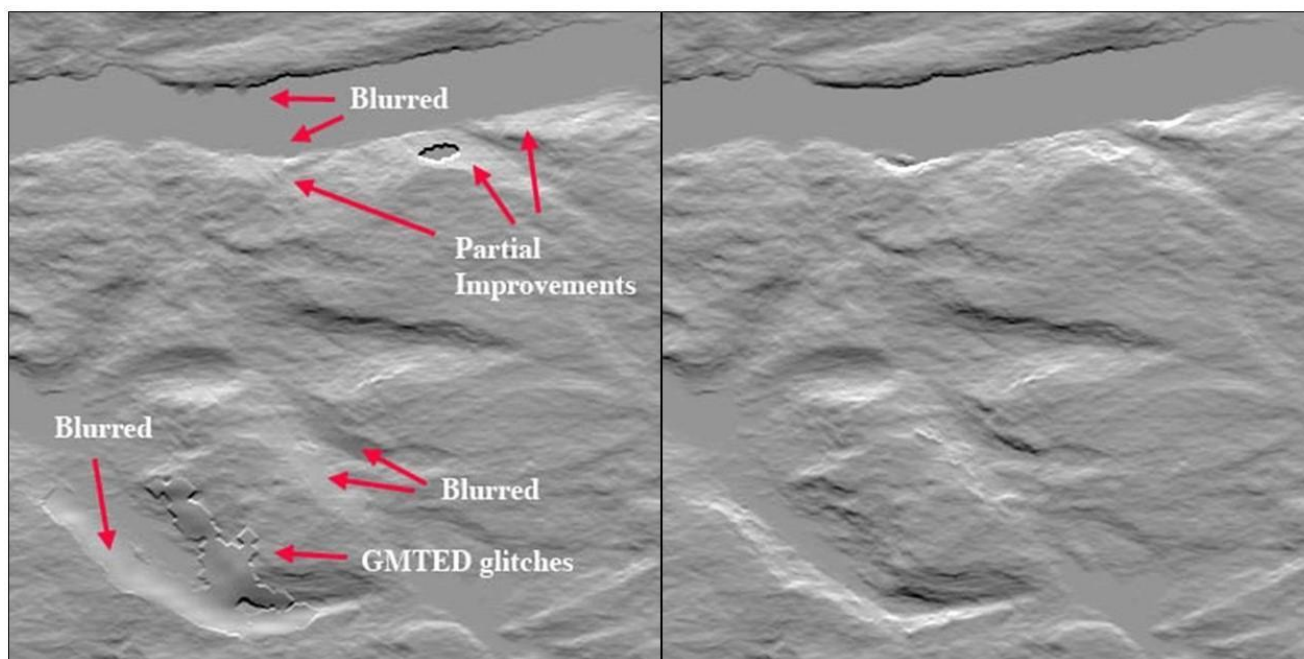

Figure 1. GDEM V3 tile N60E05, 400 by 400 pixel subarea. Left: Input GDEM with errors and artifacts, both original, and introduced in early attempt at correction; Right: Final GDEM tile after corrections as described in Section 4.2.

5. NUM File

A NUM file is provided for each tile to describe the number of images (or swaths) stacked to derive

the elevation values from ASTER (GDEM V2 and initial GDEM V3), PRISM, and SRTM. The ASTER scene count is limited here to 50 for both GDEM V2 and GDEM V3 (in some areas the actual scene count exceeds 100). The actual maximum scene count for PRISM is 54 (37 in non-polar areas) and is fully indicated. The actual maximum swath count for SRTM is 23 and is fully indicated. Some other NUM values simply indicate the data type previously used as fill sources in GDEM V2 and the initial GDEM V3 (identified by a single value). See Table 3. The NUM files are presented as single-byte (8-bit, 0-255 Digital Number (DN)) images for easy visual display. The tile size, posting interval, and geometric formats of the NUM files are consistent with the DEM files described in Table 1.

Table 3. Contents of NUM file showing number of DEM tiles used, and source of void fill. *0=Unspecified; **National Geospatial-Intelligence Agency (filled SRTM).

NUM	DEM Source
0-50	GDEM V3 (0* to 50+ scenes)
60-110	GDEM V2 (0* to 50+ scenes)
131-184	PRISM (1 to 54 scenes)
201-223	SRTM (1 to 23 swaths)
231	SRTM V3 from initial GDEM V3
232	SRTM V2 from initial GDEM V3
233	SRTM V2 from GDEM V2
234	SRTM with NGA** fill from GDEM V2
241	NED from GDEM V2 (USA)
242	NED from initial GDEM V3 (USA)
243	CDED from GDEM V2 (Canada)
244	CDED from initial GDEM V3 (Canada)
245	Alaska DEM from GDEM V2
246	Alaska DEM from initial GDEM V3
250	Interpolation

6. Key Processing Factors

The changes in the key processing factors from Version 1 to Version 2 to Version 3 are listed in Table 4.

Table 4. Key processing factors

Key processing factor	Version 1	Version 2	Version 3
Number of input scene DEMS	1,264,118	1,514,350	1,880,306
Posting interval	1 arc-second	1 arc-second	1 arc-second
Correlation kernel size	9 x 9 pixels	5 x 5 pixels	5 x 5 pixels
Minimum water body detection size	12 km²	1 km²	0.2 km²

Water body post-processing	Not applied	Applied	Separation of rivers from lakes
Filtering threshold value	40 m	40 m	40 m
Offset	-5 m offset observed	V1 offset removed	---
Release date	June 2009	October 2011	June 2019

7. Validation

Japan Spacesystems evaluated GDEM V3 against the 10 m Japan digital topographic data set. Geolocation error, compared to GDEM V2, improved from 0.11 arc-seconds (3.3 m) to 0.01 arc-seconds (0.3 m) to west; and from 0.20 arc-seconds (6 m) to 0.18 arc-seconds (5.4 m) to the north. The standard deviation of the elevation error was 12.1 m. Horizontal resolution remained at 2.4 arc-seconds (72 m). See Table 5.

Table 5. Summary of validation in Japan

		Version 1 (Kernel Size: 9 x 9)	Version 2 (Kernel Size: 5 x 5)	Version 3 (Kernel Size: 5 x 5)
Geolocation Error		0.82 arcsec to west 0.47 arcsec to south	0.11 arcsec to west 0.20 arcsec to north	0.01 arcsec to west 0.18 arcsec to north
Elevation Error	Offset	About 6 m	About 0 m	N/A
	SD	14.8 m	12.6 m	12.1 m
Horizontal Resolution		3.8 arc-sec. (114 m)	2.4 arc-sec. (72 m)	2.4 arc-sec. (72 m)

8. Data Product Access and Citation

The following tools offer options to search the LP DAAC data holdings and provide access to the data:

Bulk download: LP DAAC Data Pool and DAAC2Disk
Search and browse: NASA Earthdata Search

Citing ASTER GDEM V3 data:

NASA/METI/AIST/Japan Spacesystems, and U.S./Japan ASTER Science Team. *ASTER Global Digital Elevation Model V003*. 2018, distributed by NASA EOSDIS Land Processes DAAC, https://doi.org/10.5067/ASTER/ASTGTM.003

9. References

[1] Fujisada, H., G. B, Bailey, G. G. Kelly S. Hara, and M. Abrams, ASTER DEM performance, 2005, IEEE Transactions on Geoscience and Remote Sensing, vol. 43, no. 12, pp. 2707-2714.

[2] Fujisada, H. Urai, M. and A. Iwasaki, Advanced methodology for ASTER DEM generation, 2011, IEEE TGARS, vol. 49, no. 12, pp. 5080-5091.

[3] Fujisada, H., M. Urai, and A. Iwasaki, Technical methodology for ASTER global DEM, 2012, IEEE Transactions on Geoscience and Remote Sensing, vol. 50, no. 10, pp. 3725-3736.

[4] NASA JPL. *NASA Shuttle Radar Topography Mission Global 1 arc second*. 2013, distributed by NASA EOSDIS Land Processes DAAC, https://doi.org/10.5067/MEaSUREs/SRTM/SRTMGL1.003

[5] USGS. *USGS Alaska Digital Elevation Models (DEM) 5 meter*. 2013, distributed by USGS *The National Map*.

[6] National Resources Canada. *Canadian Digital Elevation Data (CDED) 3 arc second*. 2008, distributed by Open Government of Canada GeoBase.

[7] USGS. *Global Multi-resolution Terrain Elevation Data 2010 7.5 arc second.* 2010, distributed by USGS EarthExplorer.

[8] JAXA. *ALOS Global Digital Surface Model 1 arc second.* 2017, distributed by JAXA Earth Observation Research Center.

[9] Grohman, G., G. Kroenung, and J. Strebeck, 2006, Filling SRTM voids: The Delta Surface Fill method. Photogrammetric Engineering and Remote Sensing, v. 72, no. 3, p. 213-216.

10. Acknowledgement

Appendix 1

In simple terms, the original Delta Surface Fill method is intended to create a void-free DEM from (1) a primary DEM that has voids and (2) a secondary DEM that does not have voids. The secondary DEM fills the voids seamlessly by being adjusted vertically to compensate for height differences (the delta) between the DEMs, with particular focus on the primary DEM's void edges. Elevations of the secondary DEM within the voids of the primary DEM (where deltas can only be estimated) are adjusted vertically by deltas interpolated from those void edges. Thus, a full delta surface (the DEM difference) is calculated as a simple subtraction where outside the voids, and it is filled by interpolation within the voids. That void-free delta surface is the spatially variable vertical shift that is applied to the filler DEM as it fills the voids of the primary DEM.

As implemented for some steps (not the final step) for NASADEM, the delta surface has voids not only from the primary DEM but also from the secondary (filler) DEMs. This often means that some elevations (including void edges) in the primary DEM correspond to voids in the secondary DEM. This is not a severe problem because, unless the DEMs are badly corrupted, all of the delta surface values across a region should be nearly a constant. The delta surface measures general vertical differences between the DEMs (such as reference datum errors, which are spatially constant), various possible warps, and local vertical differences between the DEMs (associated with measurement errors of individual or neighboring pixels, thus having high spatial frequencies and no widespread trends). In

short, estimating delta surfaces for voids in the primary DEM is usually performed by interpolation of the delta surface from the edges of those voids. But if it is performed by interpolation from further away, namely at the edge of the void of the filler DEM, there is usually no large adverse impact. The fill may be somewhat less "seamless" at the edge of the void in the primary DEM, but that "seamlessness" may just have been corruption of the fill to better match errors at the void edge. It may look better (smoother) but be less correct in terms of actual elevations. Thus, applying the Delta Surface Fill method with a filler-DEM that has voids does work, but it will (of course) leave remnant voids where both DEMs are void.

The delta surface (as with nearly any difference image) is typically quite noisy. The vast majority of the elevation signal is cancelled and only differences (e.g., errors and possibly temporal differences) in the elevation measurements remain. Systematic errors (reference datums and warps) will remain, and these are what the delta surface is intended to extract and then suppress in the DEM merger. However, random errors also exist pixel-by-pixel or over small areas. This may be especially true at void edges next to pixels that were voided because they were clearly erroneous or at least unreliable. Interpolation from void edge pixels can therefore result in a delta surface fill that is particularly noisy. To suppress this, a 5 by 5 pixel median filter was applied to the non-void pixels (only near voids, for speed). Interpolation across the delta surface voids then proceeded using these filtered void-edge pixels.

However, the delta elevations are typically still quite noisy, so an interpolation method is needed that suppresses local noise and keeps it local. Consequently, a repetitive edge growing interpolator was used. Pixels in the void directly adjacent to the void edge were interpolated, and then the void pixels next to those were interpolated from the first interpolated pixels. The edge growing interpolator was run for five iterations. This greatly smoothed the void fill. For speed in global processing, remaining void pixels used direct interpolation and skipped edge growing.

In both the edge growing interpolator and the interpolator without edge growing, an inverse square root of distance interpolator that looked in 16 directions (north, south, east, west, and approximately west-northwest, northwest, north-northwest, etc.) was applied. Using the inverse square root of distance may be unique. Interpolators often use the inverse square (not square root) of distance to more heavily weight nearby reference points, especially the single nearest reference point. But to some degree the opposite approach was desired. To de-emphasize noise in the very nearest reference points. Distant pixels are generally less relevant in most interpolations. But recall that the delta surface generally measures a fairly uniform value (the elevation signal cancels out). Distant reference pixels are more scattered and therefore less redundantly subject to a single noise source. Giving them extra weighting helps to reduce noise. This is particularly true in the edge-growing interpolator because typically half of the 16 look directions find pixels that are only a very few pixels away, and close pixels (due to their quantity) already get heavily weighted because of that. The inverse square root of distance formula helps balance the weighting of reference points around the void.